Journal of Materials Chemistry

Cite this: *J. Mater. Chem.*, 2012, **22**, 12907

www.rsc.org/materials

PAPER

High strength composite fibres from polyester filled with nanotubes and graphene†

Umar Khan, Karen Young, Arlene O'Neill and Jonathan N. Coleman*

Received 28th March 2012, Accepted 21st May 2012
DOI: 10.1039/c2jm31946b

We have prepared composite fibres based on the polyester, polyethylene terephthalate (PET), filled with both single walled nanotubes and graphene by a combination of solution and melt processing. On addition of ≤2 wt% filler we observe increases in both modulus and strength by factors of between ×2 and ×4 for both fillers. For the nanotube-based fibres, the mechanical properties depend strongly on fibre diameter due to a combination of defect and nanotube orientation effects. For the graphene filled fibres, the modulus is approximately invariant with diameter while the strength is defect limited, scaling weakly with diameter. Using this production method, the best fibre we prepared had modulus and strength of 42 GPa and 1.2 GPa respectively (2 wt% SWNT). We attribute this reinforcement predominately to the dispersion quality resulting from the solvent exfoliation of both nanotubes and graphene. In general, marginally better reinforcement was observed for the nanotube filled fibres. However, because of the low cost of graphite, we suggest graphene to be the superior reinforcement material for polymer fibres.

Introduction

Synthetic polymeric fibres are a very important part of modern life and are used extensively in applications in areas such as textiles, packaging and medical technology. Their widespread use is largely due to their high strength and low density but also due to their durability, abrasion resistance, and chemical and environment stability. Polyester fibres are probably the most widespread form of synthetic polymeric fibre,[1] while the most common polyester fibres are produced from poly(ethylene terephthalate) (PET).[2] PET fibres are most widely used in textiles and can be produced with Young's modulus, strength and tensile toughness up to ~10 GPa, ~1 GPa and 200 MJ m^{-3} respectively.[3] In addition, these fibres are reasonably ductile with strain at break usually varying in the range ~20 to 100%. (We note that bulk PET is generally less stiff, less strong and can be more ductile.)[4] The strongest polyester fibre ever reported was produced from polyethylene naphthalate (PEN) and had modulus, strength and ductility of 26 GPa, 1.3 GPa and 7.6% respectively (taking the density to be 1.35 g cm^{-3}).[5] However, while these mechanical properties are impressive, they cannot compare to high performance rigid rod polymeric fibres such as ultra-high molecular weight polyethylene (Dyneema®), polyparaphenylene terephthalamide (Kevlar®) and polypyridobisimidazole (PIPD) which can display modulus and strength as high as 330 GPa and 4 GPa respectively.[6] However, one advantage of polyester fibres is that they can be melt-spun, cheaply and in large quantities. Thus, there would be significant advantages to modifying existing polyesters to produce fibres with enhanced mechanical properties.

For any fibre, the mechanical performance can be partially summarised by the breaking force, F_B, which can be achieved for a given linear mass density, M/L. These quantities are related by $F_B = (\sigma_B/\rho)M/L$, where σ_B and ρ are the tensile strength and density respectively. This means that to maximise the breaking force for a given mass of polymer, σ_B/ρ must be maximised. This is an important goal; increasing σ_B/ρ would mean that less polymer is required for a given application (*i.e.* given F_B). For example, doubling σ_B/ρ would mean only half as much PET would be required to produce a given length of fibre with a given performance. As global production of PET fibre alone was ~30 million tonnes in 2010 (http://www.textileworld.com), achieving this goal would have a huge impact on plastics usage and result in considerable cost savings.

Over the last decade, a lot of work has been done to reinforce polymeric fibres with nanoscale fillers.[7–9] When stiff, strong, rodlike (or planar) fillers are added to polymers, the mechanical properties can be improved dramatically. The simplest possible model to describe this reinforcement is the rule of mixtures (as modified by shear lag theory) which predicts that the fibre modulus, Y, and strength, σ_B, depend on the filler volume fraction, V_f, by:[10,11]

$$Y = (\eta_o \eta_{LY} Y_R - Y_P)V_f + Y_P \quad (1)$$

Centre for Research on Adaptive Nanostructures and Nanodevices and School of Physics, Trinity College Dublin, Dublin 2, Ireland. E-mail: colemaj@tcd.ie

† Electronic supplementary information (ESI) available. See DOI: 10.1039/c2jm31946b

$$\sigma_B = (\eta_o \eta_{L\sigma} \sigma_R - \sigma_P) V_f + \sigma_P \quad (2)$$

here the subscripts R and P refer to the reinforcing filler and the polymer respectively. In addition η_{LY}, $\eta_{L\sigma}$ and η_o are efficiency factors which vary between 0 and 1 and correct for the effects of nanotube length and orientation respectively (*N.B.* different forms of the length efficiency factor are used for modulus and strength *i.e.* η_{LY} and $\eta_{L\sigma}$ respectively).[12,13] These expressions mean that the rate of increase in both fibre modulus and strength with filler content have upper limits given by $dY/dV_f \leq Y_R$ or $d\sigma_B/dV_f \leq \sigma_R$.

Due to their intrinsically high stiffness and strength, one of the most exciting filler materials of recent years has been carbon nanotubes. These high aspect ratio carbon cylinders have diameters of ~1 nm, lengths of ~1 micron and display superlative mechanical properties with modulus and strength up to 1 TPa and 50–150 GPa respectively.[8,14–19] Some significant successes have been achieved by reinforcing polymers with carbon nanotubes.[8] Polymer–carbon nanotube composite fibres have been produced using a range of matrices and spinning methods and in some cases have achieved exceptional mechanical properties, with a number of papers describing composite fibres with strength in excess of 1 GPa.[13,20–24] However, in many cases the key to such impressive results has been the quality of the nanotube dispersion which is usually achieved through solution processing. This often means that the fibres have been formed from solution using methods such as coagulation spinning.[25] This is unfortunate as many commercial plastic fibres are melt processed; it has proved more difficult to produce excellent composite fibres from the melt than from solution.[8]

Surprisingly few papers have reported the reinforcement of polyester fibres. A small number of papers have described the reinforcement of PET fibres with carbon nanofibres[26] or organoclays[27] with limited improvements in mechanical properties. In addition, some papers have reported the production of nanotube–PET composite fibres.[28–30] Of these, the most impressive results were those of Anand *et al.* who prepared composite fibres by melt compounding, followed by spinning and drawing.[28] They obtained fibres with a modulus and strength of 15.9 GPa and 712 MPa respectively, significantly better than their measurements for the pure polymer.

However, we believe that it is possible to build on this work to generate fibres with significantly higher stiffness and strength at reduced cost. It is known that some nanotubes are present as large aggregates when melt mixed into PET.[30] This is probably a result of incomplete exfoliation during mixing. Such aggregates act to concentrate stress and can instigate failure. We propose to address this issue by first exfoliating the nanotubes in a solvent before mixing into the PET melt. This should lead to a uniform composite with well dispersed nanotubes and minimal aggregates. Another problem with using nanotubes as a filler, is that those types of nanotube with high strength (*i.e.* single walled nanotubes) tend to be extremely expensive (~$500 per g). We propose to resolve this issue by using solvent exfoliated graphene as a filler material. Using these strategies we demonstrate the production of composite fibres with high stiffness and strength, using a filler (graphene) exfoliated from a starting material which costs as little as ~$5 per kg.

Experimental procedure

Composite melts were produced by adding solvent-dispersed, exfoliated single walled nanotubes or graphene to a PET melt while stirring. After solvent evaporation, a uniform melt was obtained with no visual evidence of aggregates. The procedure is described in detail below.

Graphite powder (Aldrich product number 332461, batch number 06106DE) was dispersed in *N*-methyl-2-pyrrolidone (NMP, Aldrich) at an initial concentration of 3 mg ml^{-1} (1800 mg in 600 ml) by bath sonication (Branson1510E-MT) for 144 hours using methods described recently.[31,32] In order to produce a more concentrated dispersion,[33] this was then filtered on a porous nylon membrane (Sterlitech, pore diameter 0.45 μm). The deposited graphene was then re-dispersed in 15 ml of fresh NMP by bath sonication for a further 24 h. This dispersion was then centrifuged at 1000 rpm for 45 min and the supernatant collected.

SWNTs (HiPCO, Unidym) were dispersed in NMP at an initial concentration of 5 mg ml^{-1} using a sonic tip processor (GEX600, 120 W, 60 kHz, flat head probe) operated in pulsed mode (9 s on/9 s off) for 16 h.[34–36] The resulting dispersion was further sonicated in a sonic bath for 4 hours immediately before use to ensure a good quality dispersion. The dispersion was not centrifuged at any time. Under these conditions, we expect the nanotubes to be arranged in bundles with diameters ~10 nm and lengths of ~1 μm.[36]

The dispersed concentration was estimated by filtering 2 ml of dispersion through a nylon membrane which was then dried in an oven (60 °C) for an hour. The filtrate mass was found by careful weighing, yielding concentrations of 5mg and 9 mg ml^{-1} for nanotube and graphene dispersions respectively. These stock dispersions were then diluted to produce a series of dispersions with a range of concentrations.

A 125 μm thick sheet of PET weighing 1 g (ST505 Melinex PET made by Dupont Teijin, measured mechanical properties $Y = 1.3$ GPa, $\sigma_B = 148$ MPa, $\varepsilon_B = 150\%$) was cut into pieces, placed in a beaker on a hotplate (~200 °C) and allowed to melt over the course of approximately 10 min. Composite melts were produced by adding a dispersion of nanotubes/graphene containing a given nanotube/graphene mass in a given volume of NMP to the PET melt in order to achieved the desired polymer/filler mass fraction. In all cases the same volume of dispersion was added so that each melt would have been exposed to the same volume of solvent. The nanotube/graphene mass was varied by controlling the concentration. The mixture was constantly stirred to give a homogeneous liquid. After approximately 10 min of heating, the NMP had evaporated to give a composite melt. However, we note that it is likely that small amounts of residual NMP remained in the melt. The mass fraction of the composite is controlled by the mass of nanotubes/graphene added and the PET mass. Nanotube and graphene filled composite melts were prepared at mass fractions (0.5 wt%, 1 wt%, 2 wt%) and (0.25 wt%, 0.5 wt%, 1 wt%, 4 wt%) respectively.

Fibres could be formed from either a PET or composite melt by inserting a fine needle to which the melt adhered strongly. The needle was drawn out of the melt at a rate of ≈40 cm s^{-1} to give a fibre. The fibres were left to cool in ambient conditions for a minimum of 1h before drawing to the maximum possible draw

ratio before failure. Interestingly, while the PET fibres could only be drawn to ~200%, the composite fibres could generally be drawn considerably further: SWNT fibres – (0.5 wt%, 400% draw), (1 wt%, 250%), (2 wt%, 400%) and graphene fibres – (0.25 wt%, 370%), (0.5 wt%, 350%) (1 wt%, 400%), (4 wt%, undrawable). This is in contrast to the experience of Anand *et al.*[28] and Mun *et al.*[30] who found that the maximum draw ratio either remained constant or was reduced in the presence of nanotubes in the vast majority of cases.[28,30] In addition, the 1 wt % nanotube fibres and 0.5 wt% graphene fibres were drawn to a range of draw ratios (and so a range of final diameters). The fibres were drawn while cool and released immediately afterward. In all cases, they retained all of the drawn length.

Using this procedure, between 4 and 23 fibres were produced for each volume fraction of both nanotubes and graphene. After drawing, the fibre diameters were measured at typically 3 positions along their lengths using a profilometer (Dektak 6M Stylus Profiler). The diameter variance along a fibre was typically small (<10%). The mean diameter varied from 3 to 19 μm for the nanotube composites and 5 to 20 μm for the graphene composites. We note that using this procedure we have no control over the fibre diameter before drawing but some control of the diameter after drawing.

Tensile testing was performed on all fibres with a Zwick Z100 tensile at a strain rate of 5 mm min^{-1}. In all cases the gauge length was 1 cm. SEM measurements were performed using a Carl Zeiss Ultra Plus Field Emission Scanning Electron Microscope. The nanotube/graphene mass fraction was converted to volume fraction assuming the densities: $\rho_{PET} = 1300$ kg m^{-3}, $\rho_{SWNT} = 1800$ kg m^{-3} and $\rho_{graphene} = 2100$ kg m^{-3}.

Results and discussion

PET–nanotube fibres: volume fraction dependence

The processing procedure used in this work resulted in large set of PET–nanotube fibres with a range of volume fractions and diameters. SEM images of a selection of these fibres are shown in Fig. 1. As shown in Fig. 1A the fibre diameter is uniform and the cross-section relatively circular (Fig. 1B). In addition, the sidewalls are relatively smooth and well defined (Fig. 1C). No signs of nanotube aggregates were observed in any fibres suggesting dispersion quality to be high. Shown in Fig. 1D is a fracture surface of a broken fibre. Close to the centre of the fibre, a number of SWNT bundles can be seen protruding. This suggests that the fracture mechanism is by nanotube pullout. This implies that the nanotubes used here are shorter than the critical length (*i.e.* the minimum filler length required for enough stress to be transferred to the filler to result in breakage of the filler particles).[12] This usually means that the fibre strength will not be limited by the nanotube strength but rather by the polymer–nanotube interface.[12]

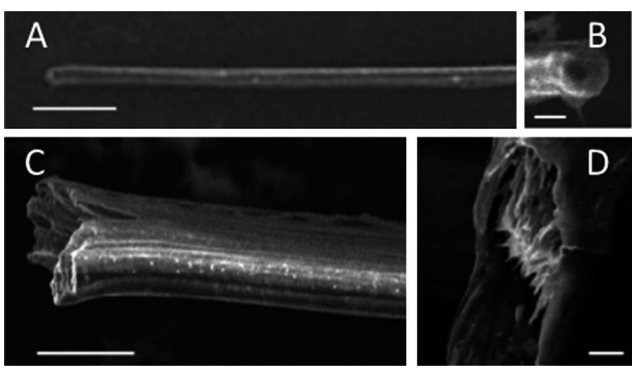

Fig. 1 SEM images of melt processed PET–SWNT fibres. The scale bars are (A) 20 μm, (B) 2 μm, (C) 10 μm and (D) 1 μm.

Stress–strain measurements were made for all fibres. For composites, the most fundamental question is how the mechanical properties scale with filler content. The measured fibres (all volume fractions and draw ratios) were divided into subsets where the fibres had with similar diameters (maximum deviation from mean diameter was ~10%). Note that less than half of the total fibres could be grouped into such subsets. This allowed the study of the effect of nanotube volume fraction on mechanical properties without any contribution from varying fibre diameter. This is critical as the mechanical properties of fibres can vary strongly with fibre diameter.[23,37–42] Shown in Fig. 2A are stress–strain curves for a PET fibre and composite fibres with 0.36 vol%, 0.72 vol% and 1.4 vol% SWNT. In all cases the fibres were very close to 5 μm in diameter. The measured mean modulus and strength of this PET-only fibre was 4 GPa and 420 MPa respectively. We note that these values are lower than expected for high quality PET fibres. However, we attribute this to the crude nature of our fibre formation methodology and note that it may suggest the presence of residual NMP. We anticipate

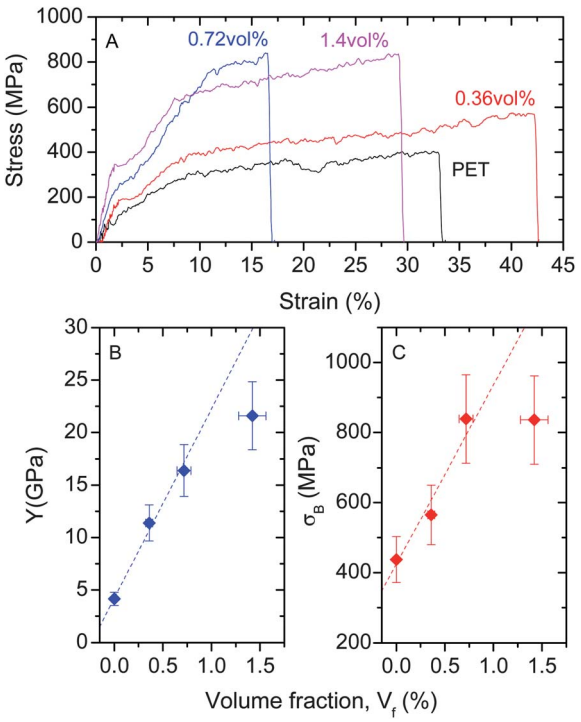

Fig. 2 Mechanical properties of PET–SWNT fibres with diameter $D \approx 5$ μm as a function of nanotube volume fraction. (A) Stress–strain curves. (B) Young's modulus. The slope of the straight line is $dY/dV_f = 1805 \pm 150$ GPa. (C) Ultimate tensile strength. The slope of the straight line is $d\sigma_B/dV_f = 51 \pm 12$ GPa.

significant improvements on moving to more advanced fibre production techniques. On addition of the nanotubes the modulus and strength increase significantly. We can quantify the increases in modulus, Y, and strength, σ_B, by plotting them as a function of volume fraction, V_f, in Fig. 2B and C. The modulus increases from 4 GPa for PET to 22 GPa for the 1.5 vol% sample. The initial portion of this curve is linear with slope $dY/dV_f = 1805 \pm 150$ GPa. This is significantly beyond the upper limit of 1000 GPa set by the intrinsic nanotube modulus and the rule of mixtures,[8,11,12,43] indicating that an additional component of reinforcement is present. This is not unusual, with nanotube-nucleated crystallinity a common cause.[44,45] When polymer crystallinity is induced by the filler, the degree of crystallinity tends to scale linearly with the nanotube content. Because the crystallites are both stronger and stiffer than the amorphous polymer, their presence acts to reinforce the composite over and above what would be expected from the presence of nanotubes alone.[45] In fact, this is a reasonable explanation as nanotube-induced crystallinity has been observed in PET–nanotube composites.[29] However, we were unable to test for this induced crystallinity in these fibres due to their small diameter and the low quantity of material produced per draw.

Similarly, the strength increases from 420 MPa for PET to 820 MPa for the 1.5 vol% sample. Again, the initial portion of this curve is linear with slope $d\sigma_B/dV_f = 51 \pm 12$ GPa. While this value is not beyond the upper limit of ~50 to 150 GPa set by the intrinsic nanotube strength and the rule of mixtures,[8,43] it is high compared to the majority of nanotube reinforced composites.[46] Because nanotubes are often shorter than the critical length (as is the case here),[12] composite strength is usually much lower than if it was limited by the nanotube strength.[8,43] Usually, the strength increase is limited by either defects[23] or the shear strength of the polymer–nanotube interface (or the polymer shear strength depending on which is smaller).[43,44] The large value of $d\sigma_B/dV_f$ suggests that defects don't dramatically affect the strength or that the interfacial/polymer shear strengths are relatively large. Alternatively, nanotube nucleated crystallinity may contribute strongly to the reinforcement.[44] We note that both strength and modulus behaved similarly for other fibre diameters as shown in the ESI†.

We also measured the strain at break, ε_B, to be relatively invariant with nanotube volume fraction, remaining between 20 and 40% for almost all volume fractions for each diameter set. The same behaviour was observed for the tensile toughness, T, (energy per unit volume required to break the fibre) which was typically between 75 and 175 MJ m^{-3} for most samples (see ESI†).

PET–nanotube fibres: diameter dependence

We can summarise the entire dataset by plotting each mechanical parameter (Y, σ_B, ε_B and T) as a function of fibre diameter as shown in Fig. 3. Both modulus and strength increase with decreasing fibre diameter. The highest modulus and strength observed were 42 GPa and 1.2 GPa, both for a 3.7 μm diameter fibre. Recently, it was shown that both modulus and strength of polymer–nanotube composite fibres scale with fibre diameter as power laws;[23] $Y \propto D^{-\alpha}$ and $\sigma_B \propto D^{-(\alpha+\beta)}$ (we note that in ref. 23, these exponents were described using different symbols). The

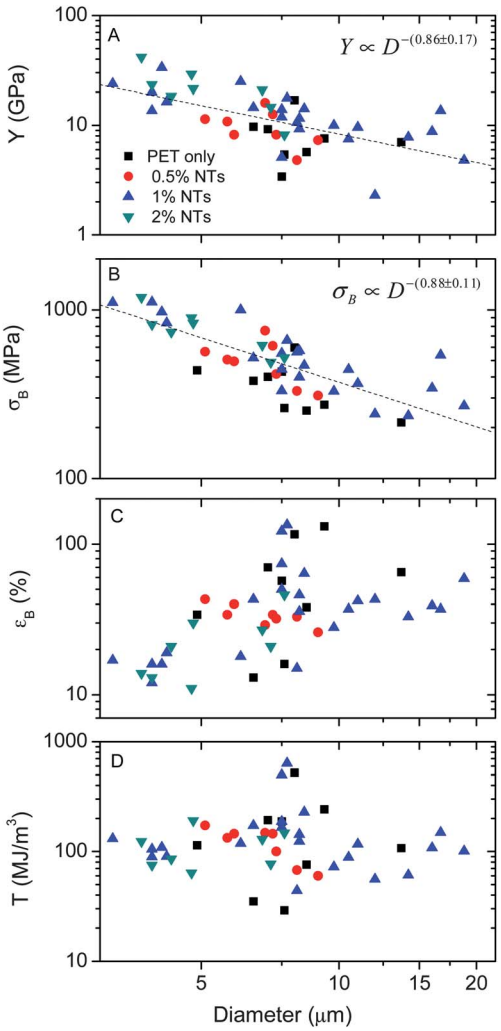

Fig. 3 Mechanical properties of PET–SWNT fibres as a function of fibre diameter. For a given fibre the typical spread in the diameter is <10%. (A) Young's modulus, (B) ultimate tensile strength, (C) strain at break and (D) tensile toughness. In (A) and (B) the dashed lines are power law fits to the entire dataset. The nanotube contents are given as wt%.

diameter dependence of the modulus is controlled only by changes in nanotube orientation with fibre diameter (as described by α). The origin of this behaviour lies in the fact that the orientation efficiency factor given in eqn (1) has been shown to scale with fibre diameter as a powder law.[23] This manifests itself as a power law dependence of modulus on diameter. However, the diameter dependence of the strength is controlled by a combination of orientation effects and surface defects. In the presence of defects it is known that the strength scales with fibre diameter as a power law where the exponent, β, is defined by the defect distribution.[23] Thus, combining the effects of defects and orientation results in the power law behaviour given above. For polyvinyl alcohol fibres reinforced by single walled nanotubes, $\alpha \approx 0.6$ while $\beta \approx 0.3$.[23] We note that smaller values of these exponents (*i.e.* α, $\beta \rightarrow 0$) mean weaker diameter dependences.

We have tested for this behaviour here by fitting the entire modulus and strength *versus* diameter datasets to power laws. We find reasonable agreement in both cases with $\alpha = 0.86 \pm 0.17$ and $\alpha + \beta = 0.88 \pm 0.11$, consistent with $\beta \leq 0.3$. We can

conclude from this that the observed diameter dependence is entirely consistent with this defect/orientation model. However, it is likely that the orientation controlled diameter dependence here is slightly stronger and the defect controlled diameter dependence slightly weaker than that observed previously.

The strain at break as a function of fibre diameter is shown in Fig. 3C. In general the strain at break tends to increase with increasing D, from ~10% to ~70% as D is increased from 4 to 18 μm. Interestingly there appears to be a peak in the strain at break for $D \approx 8$ μm where ε_B reaches 130%. The origin of this remains unclear. Shown in Fig. 3D is the tensile toughness as a function of D. This remains relatively flat at ~100 MJ m^{-3} but shows signs of a peak again around $D \approx 8$ μm. The highest value obtained was 637 MJ m^{-3} for composites containing 1 wt% nanotubes. This is relatively large compared to tough materials such as Kevlar and dragline spider silk (50 MJ m^{-3} and 150 MJ m^{-3}).[47] However, it is worth noting that in our case, the toughness is attained at relatively large ductility *i.e.* >100%.

PET–graphene fibres

Polymer–nanotube composite fibres are relatively straightforward to prepare and have been known for over 10 years.[48] In contrast, polymer–graphene fibres have not been reported to date. Like nanotubes, graphene is a promising filler due to the exception mechanical properties of monolayer graphene which has been reported at $Y \approx 1$ TPa and $\sigma_B \approx 130$ GPa.[49] While a number of papers have reported bulk composites based on chemically modified graphene as a filler,[50–57] in general the level of reinforcement achieved has been significantly below that predicted by the rule of mixtures.[11] This is probably due to a combination of the relatively poor mechanical properties of chemically modified graphene[58] and the fact that reasonably large graphene flakes are required to achieve effective reinforcement.[59,60] However, it has recently been shown that high quality, defect free graphene with relatively large flake size can be produced by exfoliation of graphite in solvents or surfactant/polymer solutions.[32,35,60–69] Here, we use a solvent-based dispersion and exfoliation method recently pioneered in our group.[31–33] This method results in dispersions of few layer graphene flakes with mean length, width and thickness (in this case) of 1.1 μm, 0.51 μm and 4.6 layers respectively. Raman spectroscopy shows the flakes to be relatively free of basal plane defects (see ESI† for more detail). As a result, we expect them to have mechanical properties approaching that of monolayer graphene. Previous work has shown such defect free flakes to be excellent reinforcing fillers.[60,69] This exfoliation method can be combined with the polymer–nanotube fibre formation method described above to prepare high quality polymer–graphene fibres.

PET–graphene fibres: volume fraction dependence

Shown in Fig. 4 are SEM images of PET–graphene fibres. Like the PET–nanotube fibres, they are uniform in diameter, have smooth, well defined walls and a circular cross-section. Again, no signs of aggregates were observed suggesting dispersion quality to be high.

Shown in Fig. 5A are stress–strain curves for a subset of PET–graphene fibres with $D \approx 13$ μm. Here both modulus and strength increase with graphene content while the strain at break tends to fall off. The modulus increases approximately linearly with graphene volume fraction from ~7 GPa to ~16 GPa for the 0.3 vol% sample. The rate of increase is $dY/dV_f = 2100 \pm 1300$ GPa. Similarly the strength increases linearly with graphene volume fraction from ~200 MPa to ~640 MPa for the 0.3 vol% sample with a rate of increase of $dY/dV_f = 145 \pm 15$ GPa. Again, these rates are at the upper limit of what might be expected from the intrinsic properties of graphene and the rule of mixtures, possibly suggesting the nucleation of crystallinity.[10] We note that

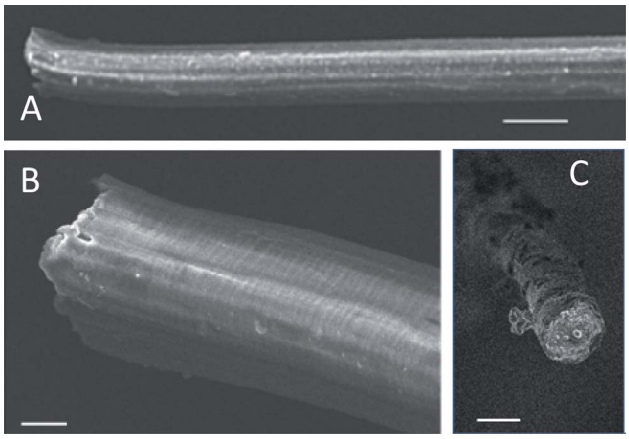

Fig. 4 SEM images of melt processed PET–graphene fibres. The scale bars are (A) 10 μm, (B) 2 μm and (C) 2 μm.

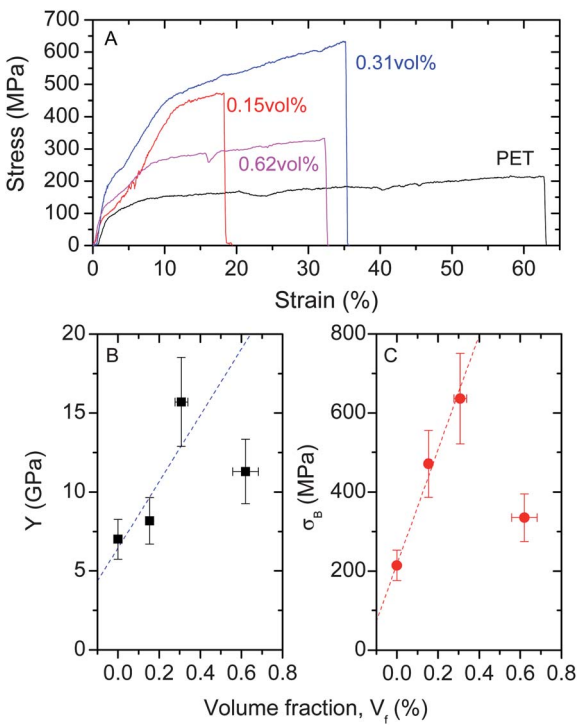

Fig. 5 Mechanical properties of PET–graphene fibres with diameter $D \approx 13$ μm as a function of graphene volume fraction. (A) Stress–strain curves. (B) Young's modulus. The slope of the straight line is $dY/dV_f = 2100 \pm 1300$ GPa. (C) Ultimate tensile strength. The slope of the straight line is $d\sigma_B/dV_f = 145 \pm 15$ GPa.

at higher volume fractions, both modulus and strength fall off dramatically, suggesting large scale graphene aggregation. Similar data were found for other fibre diameters (see ESI†).

It is worth noting that the graphene flakes used in this work are ~4 to 5 monolayers thick on average (see ESI†). At first glance such multilayer flakes might appear poor reinforcing agents due to interlayer sliding. However, Gong *et al.*[70] have shown that while such effects are present, they are mitigated by the fact that higher mass fractions can be achieved with multilayer graphene. In fact it has been shown that the most effective reinforcement is achieved, not with monolayer graphene, but with few-layer graphene.[70]

We also measured the strain at break and toughness of our fibres as a function of graphene mass fraction (ESI†). Here, we observed significant differences compared to the PET–nanotube fibres. Both ductility and toughness fell significantly with graphene content. The strain at break fell exponentially with volume fraction from ~100% to 1–2% on addition of 4 wt% graphene. A similar reduction was observed for toughness.

PET–graphene fibres: diameter dependence

As with the PET–nanotube composites, we can achieve an overview by plotting the mechanical parameters as a function of D as shown in Fig. 6. The modulus data (Fig. 6A) are extremely scattered, hardly displaying any diameter dependence at all (*i.e.* $Y \propto D^{-\alpha}$ with $\alpha = 0.1 \pm 0.2$, fit line not shown). This is perhaps not surprising for a planar filler like graphene, as confinement due to small fibre diameter may not result in orientation as efficiently as it will for rodlike fillers. As a result the largest modulus observed was 21 GPa for a relatively large fibre with $D = 9.5$ μm.

However, the strength data in Fig. 6B does display a diameter dependence, consistent with $\sigma_B \propto D^{-(\alpha+\beta)}$ where $\alpha + \beta = 0.33 \pm 0.14$. Ultimately, this means that $\beta = 0.2 \pm 0.3$, a value entirely consistent with defect limited strength.[23] As with modulus, the strongest fibre had $D = 9.5$ μm and had $\sigma_B = 1.0$ GPa.

The strain at break data are plotted as a function of D in Fig. 6C. Here two things are of note. It is very clear that addition of graphene results in a reduction of ductility. Secondly, the peak in ductility observed previously, is much clearer here. The toughness, as shown in Fig. 6D, shows similar behaviour.

Comparison of mechanical properties with previous work on PET–nanotube composites

We can benchmark the mechanical properties found here by comparing to literature values. As mentioned in the introduction, there are only a handful of papers describing composites of PET and nanotubes. For these papers, we plot the best results in terms of strength as a function of modulus in Fig. 7. In addition, we plot the same data for all of our fibres. Of the literature data, by far the highest strength and modulus values were those of Anand *et al.*[28] who attained values of $Y = 16$ GPa coupled with $\sigma_B = 720$ MPa. By comparison, our PET–nanotube (2 wt%) and PET–graphene (0.5 wt%) composites show maximum moduli of 42 GPa and 21 GPa respectively and maximum strengths of 1.2 GPa and 1.0 GPa respectively. We suggest that our data are superior largely because we have very good dispersion of the filler in the

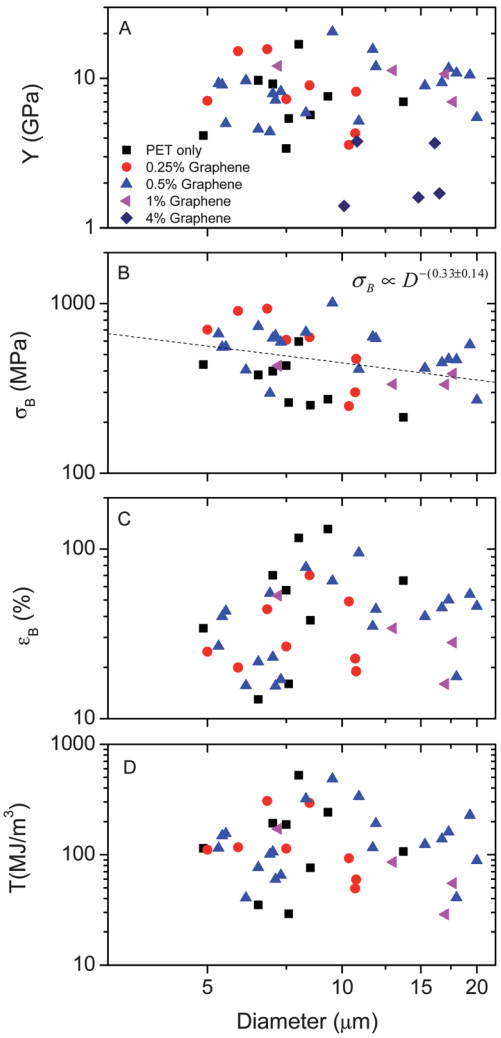

Fig. 6 Mechanical properties of PET–graphene fibres as a function of fibre diameter. For a given fibre the typical spread in the diameter is ~7%. (A) Young's modulus, (B) ultimate tensile strength, (C) strain at break and (D) tensile toughness. The graphene contents are given as wt%. The line in (B) is a power law fit to the entire dataset.

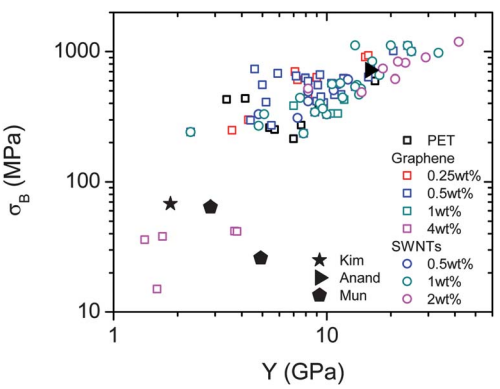

Fig. 7 Summary of strength and stiffness data for all the fibres measured in this work. For comparison, the best data from three papers in the literature are also included.

matrix (except for high graphene contents). This is almost certainly due to the fact that we disperse the fillers in NMP prior to mixing, guaranteeing minimal aggregation. In addition, it is worth noting that our best values of modulus and strength are competitive with the best polyester (*i.e.* polyester only) fibres reported to date ($Y = 26$ GPa, $\sigma_B = 1.3$ GPa for $D \approx 20$ μm).[5]

Conclusions

A method has been developed to produce PET–nanotube and PET–graphene fibres by combining solution and melt processing. These fibres have exceptional mechanical properties, similar to the best polyester fibres ever reported. For low loadings of both filler types, the modulus and strength increased linearly with volume fraction with slopes far in excess of rule of mixtures predictions, suggesting the presence of filler-induced crystallinity. For nanotube based composites, the diameter dependence of the composites suggest the modulus to be limited by nanotube orientation while the strength is limited by orientation and defects. However, for PET–graphene composites, the modulus was relatively invariant with D suggesting orientation to be relatively unaffected by diameter reduction. While the strength did depend on fibre diameter, the dependence was much weaker than for the nanotube fibres. This is consistent with orientation playing virtually no role and the strength being controlled largely by defects.

While our best composites perform better than the best polyester fibres, it is worth pointing out that our PET-only fibres are inferior to commercial PET fibres. We attribute this to the crudeness of our fibre formation procedures. We anticipate that if sophisticated fibre formation techniques were applied to the composite melts described here, significantly improved properties might be attained.

We note that the ability to successfully reinforce commodity plastics with graphene is significant for purely economic reasons. For example the cost of graphite is <€5 per kg. This means the material cost of adding 0.5 wt% (*i.e.* where the maximum mechanical reinforcement is observed) graphene to a PET fibre is <0.03 c per km for a fibre with $D = 100$ μm (*cf.* PET fibre costs ~1 c per km). As the cost of high quality SWNT is ~€500 per g, the cost per km of adding 2 wt% SWNT is approximately €100. While this cost will certainly come down, it is unlikely to fall enough to challenge the economics of graphene. In reality, the cost of exfoliation/mixing, *etc.* will increase these estimates somewhat. However, reinforcement using graphene may be economically viable in a way that nanotubes never could be.

Acknowledgements

We acknowledge financial support from Science Foundation Ireland through the Principle Investigator scheme (grant number 07/IN.7/I1772).

References

1 B. Sesto, M. Yoneyamam and H. Xiaoxiong, in *Chemical Economics Handbook Report*, SRI consulting, 2010, http://www.sriconsulting.com/CEH/Public/Reports/541.9000/.
2 *Manufactured Fibre Technology*, ed. V. B. Gupra and V. K. Kothari, Chapman & Hall, 1997.
3 S. Hansen and K. B. Atwood, in *Kirk-Othmer Encyclopedia of Chemical Technology*, John Wiley and Sons, 2005.
4 W. D. Callister, *Materials Science and Engineering an Introduction*, John Wiley and sons, 2007.
5 P. Chen, M. Afshari, J. A. Cuculo and R. Kotek, *Macromolecules*, 2009, **42**, 5437–5441.
6 H. G. Chae and S. Kumar, *J. Appl. Polym. Sci.*, 2006, **100**, 791–802.
7 O. Breuer and U. Sundararaj, *Polym. Compos.*, 2004, **25**, 630–645.
8 J. N. Coleman, U. Khan, W. J. Blau and Y. K. Gun'ko, *Carbon*, 2006, **44**, 1624–1652.
9 D. N. Saheb and J. P. Jog, *Adv. Polym. Technol.*, 1999, **18**, 351–363.
10 G. E. Padawer and N. Beecher, *Polym. Eng. Sci.*, 1970, **10**, 185.
11 J. Rosenthal, *Polym. Compos.*, 1992, **13**, 462–466.
12 D. Hull and T. W. Clyne, *An Introduction to Composite Materials*, Cambridge University Press, New York, 1996.
13 M. L. Minus, H. G. Chae and S. Kumar, *Macromol. Chem. Phys.*, 2009, **210**, 1799–1808.
14 T. Belytschko, S. P. Xiao, G. C. Schatz and R. S. Ruoff, *Phys. Rev. B: Condens. Matter*, 2002, **65**, 235430.
15 C. Y. Li and T. W. Chou, *Int. J. Solids Struct.*, 2003, **40**, 2487–2499.
16 J. P. Lu, *J. Phys. Chem. Solids*, 1997, **58**, 1649–1652.
17 J. P. Lu, *Phys. Rev. Lett.*, 1997, **79**, 1297–1300.
18 B. I. Yakobson, M. P. Campbell, C. J. Brabec and J. Bernholc, *Comput. Mater. Sci.*, 1997, **8**, 341–348.
19 M. F. Yu, B. S. Files, S. Arepalli and R. S. Ruoff, *Phys. Rev. Lett.*, 2000, **84**, 5552–5555.
20 A. B. Dalton, S. Collins, E. Munoz, J. M. Razal, V. H. Ebron, J. P. Ferraris, J. N. Coleman, B. G. Kim and R. H. Baughman, *Nature*, 2003, **423**, 703.
21 P. Miaudet, S. Badaire, M. Maugey, A. Derre, V. Pichot, P. Launois, P. Poulin and C. Zakri, *Nano Lett.*, 2005, **5**, 2212–2215.
22 M. L. Minus, H. G. Chae and S. Kumar, *Polymer*, 2006, **47**, 3705–3710.
23 K. Young, F. M. Blighe, J. J. Vilatela, A. H. Windle, I. A. Kinloch, L. B. Deng, R. J. Young and J. N. Coleman, *ACS Nano*, 2010, **4**, 6989–6997.
24 J. C. Kearns and R. L. Shambaugh, *J. Appl. Polym. Sci.*, 2002, **86**, 2079–2084.
25 B. Vigolo, A. Penicaud, C. Coulon, C. Sauder, R. Pailler, C. Journet, P. Bernier and P. Poulin, *Science*, 2000, **290**, 1331–1334.
26 H. Ma, J. Zeng, M. L. Realff, S. Kumar and D. A. Schiraldi, *Compos. Sci. Technol.*, 2003, **63**, 1617–1628.
27 J.-H. Chang, S. J. Kim, Y. L. Joo and S. Im, *Polymer*, 2004, **45**, 919–926.
28 K. A. Anand, T. S. Jose, U. S. Agarwal, T. V. Sreekumar, B. Banwari and R. Joseph, *Int. J. Polym. Mater.*, 2010, **59**, 438–449.
29 J. Y. Kim, H. S. Park and S. H. Kim, *J. Appl. Polym. Sci.*, 2007, **103**, 1450–1457.
30 S. J. Mun, Y. M. Jung, J.-C. Kim and J.-H. Chang, *J. Appl. Polym. Sci.*, 2008, **109**, 638–646.
31 Y. Hernandez, V. Nicolosi, M. Lotya, F. M. Blighe, Z. Sun, S. De, I. T. McGovern, B. Holland, M. Byrne, Y. K. Gun'Ko, J. J. Boland, P. Niraj, G. Duesberg, S. Krishnamurthy, R. Goodhue, J. Hutchison, V. Scardaci, A. C. Ferrari and J. N. Coleman, *Nat. Nanotechnol.*, 2008, **3**, 563–568.
32 U. Khan, A. O'Neill, M. Lotya, S. De and J. N. Coleman, *Small*, 2010, **6**, 864–871.
33 U. Khan, H. Porwal, A. O'Neill, K. Nawaz, P. May and J. N. Coleman, *Langmuir*, 2011, **27**, 9077–9082.
34 S. D. Bergin, V. Nicolosi, P. V. Streich, S. Giordani, Z. Sun, A. H. Windle, P. Ryan, N. P. P. Niraj, Z.-T. T. Wang, L. Carpenter, W. J. Blau, J. J. Boland, J. P. Hamilton and J. N. Coleman, *Adv. Mater.*, 2008, **20**, 1876–1881.
35 J. N. Coleman, *Adv. Funct. Mater.*, 2009, **19**, 3680–3695.
36 S. Giordani, S. D. Bergin, V. Nicolosi, S. Lebedkin, M. M. Kappes, W. J. Blau and J. N. Coleman, *J. Phys. Chem. B*, 2006, **110**, 15708–15718.
37 T. Amornsakchai, D. L. M. Cansfield, S. A. Jawad, G. Pollard and I. M. Ward, *J. Mater. Sci.*, 1993, **28**, 1689–1698.
38 A. Arinstein, M. Burman, O. Gendelman and E. Zussman, *Nat. Nanotechnol.*, 2007, **2**, 59–62.
39 H. G. Chae, Y. H. Choi, M. L. Minus and S. Kumar, *Compos. Sci. Technol.*, 2009, **69**, 406–413.
40 Y. Ji, B. Q. Li, S. R. Ge, J. C. Sokolov and M. H. Rafailovich, *Langmuir*, 2006, **22**, 1321–1328.

41 H. D. Wagner, *J. Macromol. Sci., Part B: Phys.*, 1989, **B28**, 339–347.
42 H. D. Wagner, *J. Polym. Sci., Part B: Polym. Phys.*, 1989, **27**, 115–149.
43 F. M. Blighe, K. Young, J. J. Vilatela, A. H. Windle, I. A. Kinloch, L. B. Deng, R. J. Young and J. N. Coleman, *Adv. Funct. Mater.*, 2011, **21**, 364–371.
44 J. N. Coleman, M. Cadek, R. Blake, V. Nicolosi, K. P. Ryan, C. Belton, A. Fonseca, J. B. Nagy, Y. K. Gun'ko and W. J. Blau, *Adv. Funct. Mater.*, 2004, **14**, 791–798.
45 J. N. Coleman, M. Cadek, K. P. Ryan, A. Fonseca, J. B. Nagy, W. J. Blau and M. S. Ferreira, *Polymer*, 2006, **47**, 8556–8561.
46 Z. Wang, P. Ciselli and T. Peijs, *Nanotechnology*, 2007, **18**, 455709.
47 J. M. Gosline, P. A. Guerette, C. S. Ortlepp and K. N. Savage, *J. Exp. Biol.*, 1999, **202**, 3295–3303.
48 R. Haggenmueller, H. H. Gommans, A. G. Rinzler, J. E. Fischer and K. I. Winey, *Chem. Phys. Lett.*, 2000, **330**, 219–225.
49 C. Lee, X. Wei, J. W. Kysar and J. Hone, *Science*, 2008, **321**, 385–388.
50 H. W. Hu and G. H. Chen, *Polym. Compos.*, 2010, **31**, 1770–1775.
51 L. Jiang, X. P. Shen, J. L. Wu and K. C. Shen, *J. Appl. Polym. Sci.*, 2010, **118**, 275–279.
52 S. G. Miller, J. L. Bauer, M. J. Maryanski, P. J. Heimann, J. P. Barlow, J. M. Gosau and R. E. Allred, *Compos. Sci. Technol.*, 2010, **70**, 1120–1125.
53 K. W. Putz, O. C. Compton, M. J. Palmeri, S. T. Nguyen and L. C. Brinson, *Adv. Funct. Mater.*, 2010, **20**, 3322–3329.
54 T. Ramanathan, A. A. Abdala, S. Stankovich, D. A. Dikin, M. Herrera-Alonso, R. D. Piner, D. H. Adamson, H. C. Schniepp, X. Chen, R. S. Ruoff, S. T. Nguyen, I. A. Aksay, R. K. Prud'homme and L. C. Brinson, *Nat. Nanotechnol.*, 2008, **3**, 327–331.
55 P. Steurer, R. Wissert, R. Thomann and R. Mulhaupt, *Macromol. Rapid Commun.*, 2009, **30**, 316–327.
56 X. M. Yang, L. A. Li, S. M. Shang and X. M. Tao, *Polymer*, 2010, **51**, 3431–3435.
57 X. Zhao, Q. H. Zhang, D. J. Chen and P. Lu, *Macromolecules*, 2010, **43**, 2357–2363.
58 C. Gomez-Navarro, M. Burghard and K. Kern, *Nano Lett.*, 2008, **8**, 2045–2049.
59 L. Gong, I. A. Kinloch, R. J. Young, I. Riaz, R. Jalil and K. S. Novoselov, *Adv. Mater.*, 2010, **22**, 2694.
60 P. May, U. Khan, A. O'Neill and J. N. Coleman, *J. Mater. Chem.*, 2012, **22**, 1278–1282.
61 A. B. Bourlinos, V. Georgakilas, R. Zboril, T. A. Steriotis and A. K. Stubos, *Small*, 2009, **5**, 1841–1845.
62 A. Catheline, C. Valles, C. Drummond, L. Ortolani, V. Morandi, M. Marcaccio, M. Iurlo, F. Paolucci and A. Penicaud, *Chem. Commun.*, 2011, **47**, 5470–5472.
63 A. A. Green and M. C. Hersam, *Nano Lett.*, 2009, **9**, 4031–4036.
64 M. Lotya, Y. Hernandez, P. J. King, R. J. Smith, V. Nicolosi, L. S. Karlsson, F. M. Blighe, S. De, Z. M. Wang, I. T. McGovern, G. S. Duesberg and J. N. Coleman, *J. Am. Chem. Soc.*, 2009, **131**, 3611–3620.
65 M. Lotya, P. J. King, U. Khan, S. De and J. N. Coleman, *ACS Nano*, 2010, **4**, 3155–3162.
66 D. Nuvoli, L. Valentini, V. Alzari, S. Scognamillo, S. B. Bon, M. Piccinini, J. Illescas and A. Mariani, *J. Mater. Chem.*, 2011, **21**, 3428–3431.
67 A. O'Neill, U. Khan, P. N. Nirmalraj, J. J. Boland and J. N. Coleman, *J. Phys. Chem. C*, 2011, **115**, 5422–5428.
68 S. Vadukumpully, J. Paul and S. Valiyaveettil, *Carbon*, 2009, **47**, 3288–3294.
69 U. Khan, P. May, A. O'Neill and J. N. Coleman, *Carbon*, 2010, **48**, 4035–4041.
70 L. Gong, R. J. Young, I. A. Kinloch, I. Riaz, R. Jalil and K. S. Novoselov, *ACS Nano*, 2012, **6**, 2086–2095.